



HAL
open science

A database of capture width ratio of wave energy converters

A. Babarit

► **To cite this version:**

A. Babarit. A database of capture width ratio of wave energy converters. *Renewable Energy*, 2015, 80, pp.610-628. 10.1016/j.renene.2015.02.049 . hal-01145072

HAL Id: hal-01145072

<https://hal.science/hal-01145072v1>

Submitted on 30 Apr 2019

HAL is a multi-disciplinary open access archive for the deposit and dissemination of scientific research documents, whether they are published or not. The documents may come from teaching and research institutions in France or abroad, or from public or private research centers.

L'archive ouverte pluridisciplinaire **HAL**, est destinée au dépôt et à la diffusion de documents scientifiques de niveau recherche, publiés ou non, émanant des établissements d'enseignement et de recherche français ou étrangers, des laboratoires publics ou privés.

A database of capture width ratio of wave energy converters

A. Babarit^{a,*}

^a*LHEEA Lab, Ecole Centrale de Nantes - CNRS, 1 rue de la Noe, 44300 Nantes, France*

Abstract

The aim of this study is to establish a database for the hydrodynamic performance of Wave Energy Converters (WECs). The method relies on the collection and analysis of data available in the literature. The availability and presentation of these data vary greatly between sources. Thus, extrapolations have been made in order to derive an annual average for the capture width ratio (CWR) of the different technologies. These CWR are synthesised in a table alongside information regarding dimension, wave resource and operational principle of the technologies. It is observed that CWR is correlated to operational principle and dimension. Statistical methods are used to derive relationships between CWR and dimension for the different WEC operational principles.

Keywords: Wave energy converter, capture width ratio, hydrodynamic efficiency, database.

1. Introduction

Since the early 1980s, hundreds of Wave Energy Converters (WECs) have been studied and developed. Full-scale prototypes have been tested, and technology review papers have been published (see for example [1], [2], [3], [4], [5], [6], [7], [8]). These papers usually discuss the technologies, their classifications and technical aspects (e.g. the Power Take-off (PTO) system). They do not discuss power performance of the different wave energy technologies.

Information on power performance can be found in the literature, however in general, the information provided by any given paper is limited to the one technology being investigated. A few studies have compared power performance between different technologies, but they cover a limited number of devices [9], [10], [11], [12].

* *Email address:* aurelien.babarit@ec-nantes.fr (A. Babarit)

20 Thus, the aim of this paper is to create an extensive database for the hy-
21 drodynamic performance of WECs by reviewing power performance results
22 available in the public literature. In this paper, the approach elaborates and
23 extends on the work by [13]. Power performance is quantified in terms of
24 capture width ratio (CWR), which is reported for each device in tables 7, 8
25 and 9. To identify trends, the results were classified according to WEC oper-
26 ational principle. A relationship between dimension and CWR was identified
27 and discussed in the last part of this paper.

28 It must be acknowledged that making an objective comparison of CWR
29 across WEC technologies is not an easy task. In this work, it has been
30 necessary to make assumptions and approximations in order to address issues
31 related to discrepancies in the collected data. These are discussed in section 2
32 and section 4, and are believed to be reasonable. However, it is nevertheless
33 possible that they may influence the final results in section 4. Since all
34 assumptions and approximations made have been described in detail in this
35 paper, the extent of this influence may be assessed in future work.

36 2. Methods

37 The sources for the present work are references [9] to [11] and [14] to
38 [45], which present performance results for various WECs. The performance
39 measure used and the way in which results are presented vary greatly from
40 one source to another. Thus, for the purpose of comparison, it was necessary
41 to select a common performance measure, namely annual average of CWR.
42 Note that CWR may also be referred to in the literature as ”‘non-dimensional
43 performance”’ [12].

44 2.1. CWR

45 Capture width (CW) was first introduced in 1975 by [46]. It is defined
46 as the ratio of absorbed wave power P (in kW) to the wave resource J (in
47 kW/m):

$$CW = \frac{P}{J} \quad (1)$$

48 The unit of capture width is a length in meters. It may be interpreted as
49 the width of wave crest that has been completely captured and absorbed by
50 the WEC.

51 More than capture width, it is hydrodynamic efficiency that best reflects
 52 the hydrodynamic performance of a WEC. A measure of the hydrodynamic
 53 efficiency is the CWR, obtained by dividing the capture width by a charac-
 54 teristic dimension B of the WEC - often the device width. CWR, denoted
 55 by η_1 , reflects the fraction of wave power flowing through the device that is
 56 absorbed by the device:

$$\eta_1 = \frac{CW}{B} = \frac{P}{JB} \quad (2)$$

57 Selection of a relevant characteristic dimension for B is critical in order
 58 to make CWR comparable between different wave energy devices. This is
 59 discussed further in section 2.4.

60 It is important to note that CWR relates to hydrodynamic power per-
 61 formance (energy absorption) and not economical performance (cost of en-
 62 ergy). Efficiency in the PTO system and the power conversion chain, as well
 63 as fabrication and operation costs, may be such that the most efficient de-
 64 vice hydrodynamically speaking could be the least efficient device from the
 65 perspective of cost of energy.

66 *2.2. Harmonization of power performance results*

67 Only a few of the sources present data for the annual average of capture
 68 width and wave resource J . In other cases, it is necessary to extrapolate
 69 from available results to estimate CWR. The methodology is illustrated in
 70 figure 1 and discussed in the following.

71 In some of the sources, power matrices are provided. In these cases,
 72 estimates of annual average capture width at different locations are obtained
 73 by first multiplying scatter diagrams with power matrices and then summing
 74 the power contributions from each sea state. Scatter diagrams shown in [11]
 75 were used. Linear interpolation is when the bins of the power matrix and
 76 the scatter diagram do not match.

77 In other sources, information about capture width or power absorption
 78 is provided for only a limited number of sea states. In these cases, it is
 79 necessary to estimate the power matrices as follows. First, it was assumed
 80 that power absorption is zero for sea states with peak period less than 3
 81 seconds or greater than 20 seconds. Then, linear interpolation was used to
 82 obtain power absorption as a function of the peak period. Finally, the power
 83 matrix was fully populated by scaling power absorption with the square of

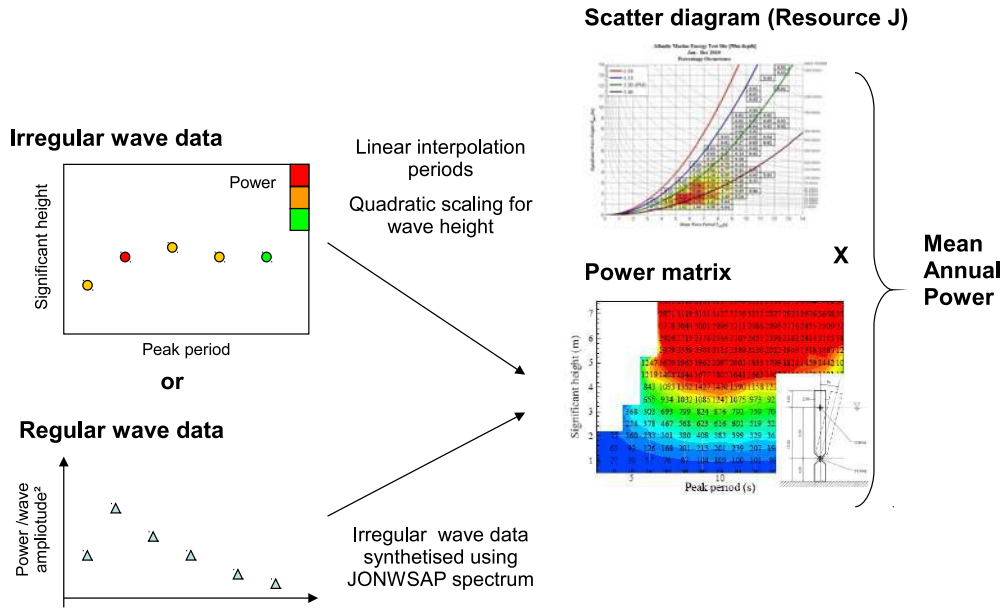


Figure 1: Outline of the methodology used for the harmonization of power performance results.

84 significant wave height. Once the power matrix was derived, annual average
 85 average capture width was calculated using the methodology explained in the
 86 previous paragraph.

87 Still other sources provide information on performance only in regular
 88 waves. In these cases, power matrices were generated, again assuming lin-
 89 earity. Power absorption in regular waves was obtained by integrating over
 90 frequency the product of Jonswap spectrum with the power absorption in
 91 regular waves. Once the power matrix was determined, annual average of
 92 capture width was determined as explained previously.

93 Finally, some sources provide data on power absorption with and without
 94 advanced control (e.g. latching control, in the case of source [22]). Only
 95 power absorption with passive control was retained in the database. This
 96 was essentially for the sake of consistency, but also because many practical
 97 challenges remain to be solved before advanced control is feasible [48], [47],
 98 [49].

99 *2.3. Classification of technologies*

100 WEC technologies may be classified by: their dimension and arrange-
 101 ment with respect to the main wave direction; their distance to shore; or
 102 their operational principle. One of the most representative classifications on
 103 the basis of operational principle was proposed by Falcão [4]. In this clas-
 104 sification, devices are grouped into three main categories: oscillating water
 105 columns (OWCs), overtopping devices or oscillating bodies (referred to as
 106 wave-activated bodies in [4]). Since oscillating bodies covers a broad range
 107 of devices, this category was divided further into floating or bottom fixed
 108 devices (the latter referred to as "submerged" in [4]); and Oscillating Wave
 109 Surge Converters (referred to as "essentially rotation" in [4]) or heaving de-
 110 vices (referred to as "essentially translation (heave)" in [4]). In this work,
 111 we follow the same classification, except that no distinction is made between
 112 floating and bottom-fixed heaving devices. Thus, oscillating bodies are clas-
 113 sified as either heaving devices (devices moving essentially in heave), fixed
 114 OWSCs (OWSCs attached to a fixed reference), or OWSCs attached to a
 115 floating reference.

116 For oscillating bodies, it is believed that this distinction between heaving
 117 and surging devices has to be made because the direction of motion is an
 118 important parameter for hydrodynamic performance. Indeed, a well-known
 119 remarkable result in wave energy conversion is that, under certain assump-
 120 tions, CWR relates only to the wavelength and the degree of freedom of the
 121 device [50], and not to its physical dimensions. Assuming (i) that linear po-
 122 tential flow theory is applicable and (ii) an axisymmetrical WEC (iii) with
 123 optimal reactive control, the theoretical maximum for the capture width is:

$$CW_{max} = \epsilon \frac{\lambda}{2\pi} \quad (3)$$

124 where λ is the wavelength and ϵ is a coefficient dependent on the pattern
 125 of the radiated wave far field, and thus on the degree of freedom. If the system
 126 is moving in heave (heaving buoy), the far field component of the radiated
 127 waves has a circular pattern (left figure in figure 2) and the coefficient ϵ is
 128 equal to 1. If the system is moving in surge and/or pitch, the wave pattern
 129 is antisymmetric (right figure in figure 2) and the coefficient ϵ is 2. The
 130 theoretical maximum for wave absorption of an axisymmetric WEC moving
 131 in surge or pitch is twice that of for the same WEC moving in heave.

132 These theoretical results highlight the importance of the radiated wave
 133 pattern on the hydrodynamic performance of a WEC; hence, a WEC classi-

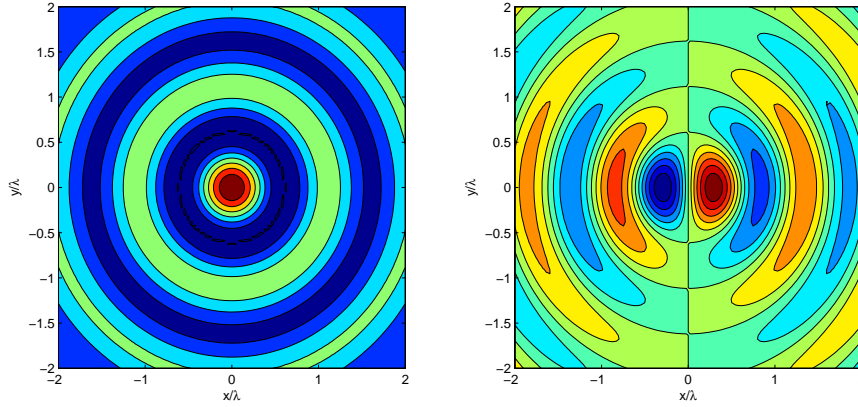


Figure 2: Far field pattern of the radiated wave for an axisymmetric device moving in heave (left graph) and in surge (right figure).

134 fication should take into account the WEC's far field radiated wave pattern.
 135 As this pattern is essentially related to the direction of motion, it represents
 136 a distinction between heaving devices and OWSCs. The latter have been
 137 further subdivided into devices attached to a fixed reference or a floating
 138 reference. Indeed, performance of floating OWSCs is considerably less than
 139 devices held to a fixed reference because the whole platform has a tendency
 140 to move as a rigid body instead of developing relative motion.

141 Figure 3 shows the archetypal device for each category. It must be ac-
 142 knowledged that in practice, devices may differ significantly from the archetype.
 143 In some examples, the operational principle may be the only relationship be-
 144 tween the device and the archetype. Thus, it was decided to sub-divide
 145 each category into those devices that are close realizations of the archetype,
 146 and those devices that are related to the category essentially by the opera-
 147 tional principle. This distinction leaves us with the following ten categories:
 148 OWCs, variants of OWCs, overtopping devices, variants of overtopping de-
 149 vices, heaving devices, variants of heaving devices, fixed OWSCs, variants of
 150 fixed OWSCs floating OWSCs and variants of floating OWSCs.

151 Note that, in this study, articulated devices such as the Pelamis or the
 152 DEXA are classified as variants of heaving devices. This is because: (i) to
 153 first order, the motion of the center of the floats is vertical, and (ii) from the
 154 hydrodynamical perspective, they can be approximated as a series of heaving
 155 buoys [51].

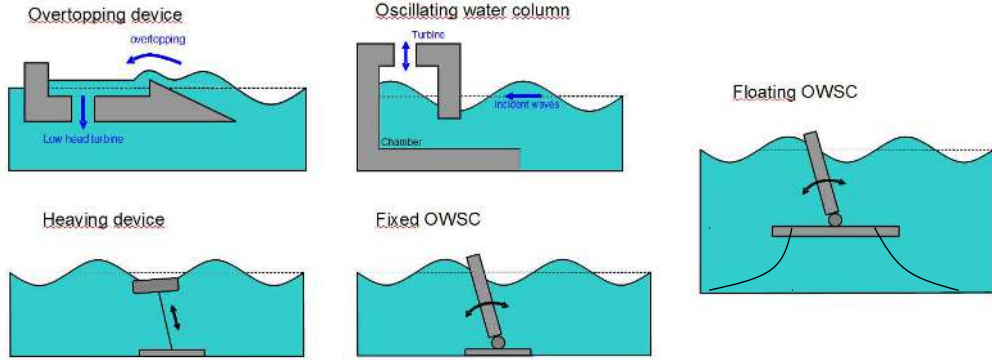


Figure 3: Illustration of the archetypal wave energy device for each category

156 Most WECs proposed so far fall into one of these ten categories. However,
 157 there are exceptions, such as wave turbines [52], [53] or flexible devices [54],
 158 [55]. These have not been considered in this study because the available
 159 information is much more limited than for the other ten categories.

160 2.4. Selection of the characteristic dimension

161 For all except heaving devices, active width was used as the characteristic
 162 dimension, B , for calculating the CWR. The definition of [12] for the active
 163 width was followed, which is based on the idea that "(...) width of all the
 164 components actively in the primary absorption process of the energy from
 165 the waves should be included". Thus, in the case of a device composed of a
 166 platform with many WECs attached to it, the performance was normalised
 167 by the number of WECs on the platform and the active width was the width
 168 of each individual WEC. In the case of devices with reflectors or a wave
 169 concentration mechanism, the active width includes the reflectors. In the case
 170 of devices inclined relative to the incoming waves, the real (not projected)
 171 width was taken into account.

172 For heaving devices, the characteristic diameter is obtained according to:

$$B = \sqrt{\frac{4A_W}{\pi}} \quad (4)$$

173 where A_W is the maximum horizontal cross-sectional area of the device, as-
 174 sumed to be the main driver for the ability of a heaving device to generate

175 waves (and thus absorb waves [1]) . Note that for vertical cylinders or floating
176 hemispheres, A_W is simply equal to the diameter.

177 *2.5. Additional information added to the database*

178 The methodology used to derive the power performance results is impor-
179 tant information to collect and retain in the database. Depending on the
180 sources, numerical or experimental modeling has been used. For experimen-
181 tal modeling, the scale varies from small-scale to full-scale prototype. This
182 information was included in the database.

183 Performance results may have been obtained by technology developers
184 or third parties. This information was also collected and retained in the
185 database, as occasionally performance results from technology developers
186 may be suspected of unreliability due to conflicting interests.

187 **3. Review of power performance results**

188 *3.1. List and discussion of sources*

189 In this section, the sources used to compile the database are presented
190 and discussed.

191 *3.1.1. Oscillating water columns*

192 Pictures of the OWC technologies discussed in this section are shown in
193 figure 4.

- 194 • Reference [14] reports experimental performance results for the NEL-
195 OWC, which is a floating terminator device composed of several OWC
196 modules mounted on a spine. The device was tested at large scale
197 in the Solent with three, five and eight modules, each module having
198 width of 1.5 m. Figure 11 of the paper presents CWR measured during
199 the sea trials as a function of the energy period. The large spread of
200 the sea trial results can be attributed to the varying properties of the
201 waves. The eight module configuration gave best performance so was
202 selected by us for estimation of the mean annual CWR. Assuming that
203 the scale of the model was 1/20, we estimated mean annual CWR to
204 be respectively 22, 27, 29, 23 % for sites with wave resource 16, 23, 27,
205 37 kW/m.

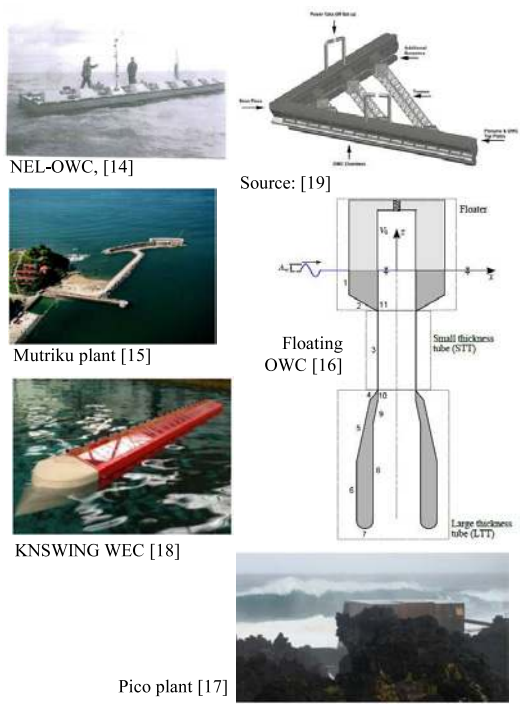


Figure 4: Pictures of the OWC technologies covered by the sources reviewed in section 3.1.1.

- 206 • [15] deals with the design and construction of the Mutriku wave power
207 plant, which is a combination of a breakwater with OWCs. The width
208 of each OWC chamber is 6 m. Power performance was assessed through
209 experiments on a 1/40 scale model of the plant, from which annual
210 average pneumatic power capture was estimated to be 175 kW for the
211 whole plant. The offshore wave resource being 26 kW/m, the mean
212 annual CWR is 7 %.

- 213 • [16] deals with performance optimisation of a floating OWC using nu-
214 merical modeling. Three configurations were investigated: (A) 8 m
215 diameter and 24 m draft, (B) 8 m diameter and 36 m draft, (C) 12
216 m diameter and 24 m draft. Other dimensions and PTO character-
217 istics were numerically optimised to maximise power absorption for a
218 site offshore Portugal. The wave resource is 31 kW/m. Mean CWR is
219 respectively 17 %, 23 % and 21 % for configurations A,B and C (see
220 table 3 of the paper). As seen in figure 4, this device differs from the
221 archetypal OWC in figure 3. Thus, it was included in the database as
222 an OWC variant.

- 223 • [17] presents power performance results for the OWC pilot plant in-
224 stalled in Pico island in the Azores. Data had been collected from
225 2005 to 2010, during which period the plant had been running for ap-
226 proximately 1 700 hours in total. As reported in the source, the mean
227 electrical power was measured to be 28 kW for an offshore wave re-
228 source of 38 kW/m. The efficiency of the Wells turbine was estimated
229 to be 31 %. The width of the plant is 12 m, thus the mean annual
230 CWR is 20 %.

- 231 • [18] presents results of experiments conducted in Cork (Ireland) for the
232 KNSWING WEC. This device is an attenuator equipped with forty
233 OWC chambers (twenty on the port side and twenty on starboard).
234 The model scale is 1/50, with a length of 3 m. It was tested both in
235 regular and irregular waves. Using this data and the scatter diagram
236 provided in the report, we calculated the mean annual CWR to be 18
237 % for a 7.5 m wide OWC and a 14 kW/m wave resource. The device
238 was classified as variant of OWC because the OWC chambers are not
239 facing the incident waves, see figure 4.

- 240 • [19] presents power performance results for a large V-shaped floating

241 WEC developed in Ireland. Each arm of the V hosts sixteen OWC
242 chambers. Power absorbed in each OWC chamber is manifolded and
243 drives one single air turbine. The length of each arm is 250 m at full
244 scale. A 1/50 scale model was tested in Cork, in Ireland. Figure 24 of
245 the paper shows the performance of the technology in regular waves.
246 Using this data, we estimated the mean annual CWR to be respectively
247 12, 14, 15, 12 % for sites with wave resource 15, 23, 27, 36 kW/m. The
248 device was classified as variant of OWC because the OWC chambers
249 are not facing the incident waves, see figure 4.

250 Power performance results for other OWC wave energy converters can be
251 found in [9], [10] and [11]. These sources are discussed in section 3.1.6.

252 3.1.2. Overtopping devices

253 Pictures of the overtopping devices discussed in this section are shown in
254 figure 5.

- 255 • Reference [20] deals with the SSG (Sea Slot-Cone Generator) wave en-
256 ergy converter, an overtopping device in which the overtopping water
257 is stored in different basins depending on the wave height. As part of
258 plans to install a 10 meter wide pilot plant in Norway, power perfor-
259 mance was investigated through experiments on a 1/60 scale model.
260 The mean annual energy production is estimated to be 320 MWh/y
261 for the Norwegian site where the wave resource is 19.5 kW/m. Accord-
262 ing to table 1 of source [20], the turbine efficiency is in the order of
263 85 % and the generator efficiency is 96 %. Thus, the mean absorber
264 power is 45 kW/m and the CWR is 23 %. This device differs from the
265 archetypal overtopping device in figure 3 because it has multiple water
266 reservoirs on top of each other. Thus, it was included in the database
267 as a variant of an overtopping device.
- 268 • [21] presents power performance results for the well-known Wavedragon
269 device. Experimental results from sea trials of a scale model at a be-
270 nign site in Nissum Bredning in Denmark were used in conjunction
271 with numerical models to derive non-dimensional performance of the
272 device. Mean annual CWR was reported to be 27 % for a site with
273 wave resource 6 kW/m and device width 65 m, and 18 % for a site
274 with wave resource 24 kW/m and device width 97 m.



Sea Slot-Cone Generator (SSG) [20]



Wavedragon [21]

Figure 5: Pictures of the overtopping devices covered by the sources reviewed in section 3.1.2.



Figure 6: Pictures of the heaving device technologies covered by the sources reviewed in section 3.1.3.

275 Power performance results for other overtopping devices can be found in
 276 [9] and [10]. These sources are discussed in section 3.1.6.

277 *3.1.3. Heaving devices*

278 Pictures of the heaving devices discussed in this section are shown in
 279 figure 6.

- 280 • Reference [22] deals with a heaving device. Inspired by the SEACAP
 281 technology developed by the Hydrocap company, the device has the
 282 form of a torus sliding along the mast of an offshore wind turbine.
 283 Mean annual power absorption was calculated for the Yeu site. Several
 284 diameters and drafts were considered for the torus, with and without
 285 latching control. For reasons explained in section 2, we retained only
 286 those results with passive control in the database. Mean CWR, calcu-
 287 lated using data from table 2 of the paper, ranges from 3 to 9 % with
 288 diameters ranging from 11 to 20 m. This is significantly smaller than
 289 the usual mean CWR for devices of that size and operational principle.
 290 This may be explained by the fact that the PTO damping coefficient

291 was optimized in order to maximize the power absorption in regular
292 waves for the resonance frequency, not in order to maximize the annual
293 energy absorption with irregular waves.

294 • [23] presents power performance results obtained using numerical mod-
295 eling for a heaving device. The WEC is a vertical cylinder with 10 m
296 diameter and 2 m height. It is a simplified version of the OPT technol-
297 ogy developed in the US. The PTO damping coefficient was optimized
298 for each sea state. The mean annual absorbed power for year 2010 was
299 estimated to be 77 kW for a site offshore Oregon in the US, where the
300 wave resource was 40 kW/m for that year. The mean annual CWR is
301 19 %.

302 • [24] presents experimental results conducted in Denmark for the DEXA
303 WEC. As explained in section 2.3, it may be classified as a variant of
304 a heaving device. A 1/30 scale model was used, with length 2.1 m
305 and width 0.81 m. Power performance results are shown in figure 13
306 of the paper. Using this data and the wave scatter diagram for Yeu
307 (having wave resource 26 kW/m), the mean annual CWR has been
308 estimated by us to be 8 % with a characteristic diameter of 22 m. The
309 characteristic diameter was calculated according to equation 4.

310 • [25] presents power performance results for the Norwegian WEC tech-
311 nology Lifesaver, a heaving device. A prototype was installed in 2012
312 in the UK. The buoy is a torus with outer diameter 16 m and inner
313 diameter 10 m. The paper reports on the experience gathered after one
314 year of full scale sea trials. It also shows the electrical power matrix
315 predicted by the numerical model of the device (table 2). According
316 to the paper, the PTO efficiency is 80 %. Using equation 4, we calcu-
317 lated the characteristic diameter of the device to be 12.5m. Hence, we
318 calculated the mean annual CWR to be 12 % for the 26 kW/m Yeu
319 site.

320 • [26] presents numerical results for the power performance of a WEC
321 inspired by the Wavestar WEC. It is composed of eight heaving buoys
322 connected to a central fixed platform. Power matrices are determined
323 for various diameters of the heaving buoys. Then, annual mean CWR
324 is calculated for coastal locations all over the world. In table 2 of the

325 paper, the average mean annual CWR is reported to be 10 % for 4 m
326 diameter configuration and 15 % for 15 m diameter configuration.

327 • [27] is the final report of a technico-economical study for four marine
328 renewable energy technologies: three current turbines and one WEC
329 (RM3). It is a heaving WEC, inspired by the OPT technology. The
330 power matrix was determined using numerical modeling and electricity
331 production calculated for a site offshore California. The wave resource
332 is 34 kW/m. The numerical model was validated against experiments.
333 Electricity production is 700 MWh at this site, assuming 80 % PTO
334 efficiency, 95 % availability and 98 % efficiency in the transmission line.
335 Thus, the mean absorbed power is 108 kW. The diameter of the buoy
336 is 20 m, thus the mean annual CWR is 16 %.

337 Power performance results for other heaving devices can be found in [9],
338 [10], [11] and [45]. These sources are discussed in section 3.1.6.

339 3.1.4. *Fixed OWSCs*

340 Pictures of the fixed OWSCs discussed in this section are shown in figure
341 7.

342 • Reference [28] is the final report of a study of the response and per-
343 formance of Salter's duck. The device reacts against a fixed reference.
344 It has three degrees of freedom: surge, heave and pitch. It extracts
345 energy from the pitch motion only. It is classified as a variant of fixed
346 OWSC. The report deals with numerical and experimental modeling.
347 Both optimal reactive control and four-term control were implemented,
348 of which only the latter is currently feasible in practice. However, even
349 the four-term control is reactive. Indeed, in figure 5.4 of the report, it
350 can be seen that one of the terms in the four-term control corresponds
351 to a negative spring in pitch. For reasons explained in section 2.2, only
352 CWR for devices with passive control are taken into account in the
353 database. Thus, this reference is not included. However, using power
354 performance results with the four-term control, i.e. graph 4 in figure
355 6.2 of the report, and according to the methodology explained in sec-
356 tion 2, mean CWR estimates for the device were calculated by us, and
357 are provided for information. They are respectively 65 %, 75 %, 79 %, 68 %
358 for a 16, 23, 27, 38 kW/m wave resource, the device width being
359 30 m.

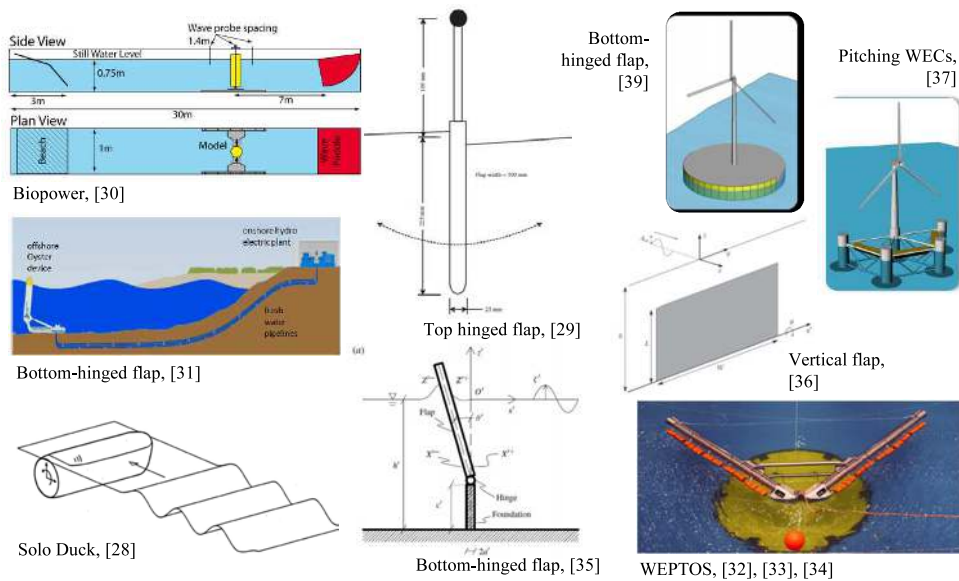


Figure 7: Pictures of the fixed OWSCs covered by the sources reviewed in section 3.1.4.

- 360
- 361
- 362
- 363
- 364
- 365
- 366
- 367
- 368
- 369
- 370
- 371
- 372
- 373
- 374
- 375
- 376
- 377
- Reference [29] reports experimental results for top-hinged flaps. Three water depths were considered: 10, 15 and 22 m. The paper shows results for the CWR in regular and irregular waves (see figures 8 and 9 in the paper). It should be noted that the characteristic dimension in the paper was the cube root of the device volume. Best performance was observed for the smallest water depth, so this was retained in the database. Using data shown in figure 8 of the paper, we calculated the mean annual CWR for a site close to Yeu island offshore the French Atlantic coast, according to the methodology explained in section 2. The wave resource is 25 kW/m, the CWR 25 %, and the width 12 m. The flaps being top-hinged, they are classified as a variant of fixed OWSC.
 - Reference [30] reports on experiments conducted on the Biopower technology in Australia. It is classified as a variant of fixed OWSC because it uses a vertical cylinder instead of a vertical flap. The technology was tested experimentally with various ballast configurations in sixteen different random sea states. The first half of the sea states are representative of winter conditions at the EMEC test site, and the

378 other half of summer conditions. Probabilities of occurrence of these
379 sea states at EMEC are given in the paper in table 1, allowing calcu-
380 lation of the wave resource in summer and winter conditions: 10 and
381 67 kW/m, respectively. Table 4 in the paper shows power performance
382 for the summer and winter seasons for each configuration tested, with
383 configuration 5 retained by us as the one with the best performance,
384 namely 41 kW in summer and 130 kW in winter. The device width
385 being 6.6m, the mean CWR is thus 45 %.

386 • Reference [31] reports power performance for a fixed OWSC in shallow
387 water depth. Figure 7 of the paper shows results of mean CWR de-
388 rived from experiments conducted in a wave tank at Queen’s University
389 Belfast in Northern Ireland. Mean CWR is 35 % for the 6 m width
390 device, increasing with width up to 65 % for a 24 m wide device. The
391 wave scatter diagram used to calculate the mean CWR is not given in
392 the paper.

393 • References [32], [33] and [34] present results of experiments of the WEP-
394 TOS technology. The WEPTOS is composed of a V-shaped platform
395 and WECs similar to Salter’s ducks. The ducks are mounted on a com-
396 mon spine on each branch of the V. They are classified as variant of
397 the fixed OWSC. A scale model was tested in 2011 in Spain and the
398 performance of the machine was measured in random waves, as well
399 as bending moments in the structure and mooring forces. Building on
400 experimental results, prototype performance at a scaling ratio of 1/15
401 was predicted in [32] at the Hanstholm site in Denmark where the wave
402 resource is 6 kW/m. The mean annual CWR is thus expected to be
403 12 % with a WEC width of 3.6 m. Using the same experimental data,
404 prototype performance at scaling ratios of 1/12, 1/15, 1/20 and 1/25
405 is predicted in [33] at the Hanstholm site (Table 2 of [33])and at site
406 in the Danish North Sea where the wave resource is 16 kW/m (Table
407 3 of [33]). In table 2 of source [34], mean annual power production is
408 reported for two other sites in Denmark, one site in France and the
409 EMEC test site in Scotland. 90 % PTO efficiency and 98 % avail-
410 ability was used in [34] according to private communication with the
411 authors. The performance results from references [32], [33] and [34] are
412 summarized in table 1.

413 • [35] is a mathematical and numerical study of a fixed OSWC in a canal.

Technology	operational principle	η_1	Dimension (m)		Resource (kW/m)
WEPTOS	Variation of fixed OWSC	8	2.9	Width	6
		10	2.9	Width	16
		12	3.6	Width	6
		12	3.6	Width	16
		19	4.8	Width	6
		15	4.8	Width	16
		15	5.4	Width	9
		25	6.0	Width	6
		19	6.0	Width	16
		32	8.3	Width	16
		22	9.6	Width	29
		25	9.6	Width	26

Table 1: Summary of performance results for the WEPTOS technology studied in [32], [33] and [34]

414 The problem is equivalent to an infinite line array of devices facing the
415 incident waves. The device is inspired by the Aquamarine/Oyster.
416 Figure 8 in the paper shows CWR for three device widths. The canal
417 width is fixed at 91.6 m. According to the method described in section
418 2, we calculated the mean actual CWR for the Yeu site, having 26
419 kW/m wave resource, to be 22 % for the 6 m wide device, 40 % for the
420 12 m device and 55 % for the 18 m device.

421 • [36] presents numerical results for the power performance of a combined
422 wind and wave energy platform. It is composed of a large floating
423 barge with twenty vertical flaps on its wave facing side and a 5 MW
424 wind turbine mounted on top of it. The floating barge is large and
425 stable, thus the WECs can be classified as a variant of fixed OWSCs.
426 The power matrix was determined using numerical modeling. Table 4
427 of the paper shows that the hydrodynamic efficiency is 72 % for a 26
428 kW/m site using the barge diameter (100 m) as the reference width.
429 Using the WEC width (10 times 16 m), the mean annual CWR is
430 calculated to be 45 %.

431 • [37] shows numerical results for the power performance of a combined
432 wind and wave energy platform. It is composed of a semi-submersible
433 platform with a 5 MW wind turbine mounted on top of it. Twelve
434 pitching WECs are installed on the wave facing braces of the platform.
435 The width of the WECs is 9 m. Based on the geometry of the WECs,
436 they are classified as a variant of fixed OWSC. The power matrix was
437 determined using numerical modeling. Table 4 of the paper shows that

438 the mean annual CWR hydrodynamic efficiency is 61 % for a 26 kW/m
439 site.

440 • [38] presents numerical results for the power performance of submerged
441 and surface piercing bottom-hinged plate wave energy converters. The
442 devices are inspired by the Aquamarine/Oyster and the AW-Energy/WaveRoller.
443 Influence of the flap height to water depth ratio and flap width to wa-
444 ter depth ratio are investigated. Figure 14 in the paper shows CWR
445 for a surface piercing flap in irregular waves (with Pierson-Moskowitz
446 spectrum) for five flap widths. Figure 19 in the same paper shows
447 CWR for a 20 m wide flap for five flap heights. The water depth is 10
448 meters. According to the method described in section 2, we calculated
449 the mean actual CWR for the Yeu site. Best performance was observed
450 for the surface piercing flap, so this was retained in the database (the
451 reference highlights the importance of having a surface-piercing device
452 for the maximization of the wave energy absorption for OWSCs). The
453 CWR estimates are 17, 36, 72 and 64 % for flap widths of respectively
454 5, 10, 20 and 50 meters and for a 26 kW/m site.

455 Power performance results for other OWSCs can be found in [11], [44]
456 and [45]. These sources are discussed in section 3.1.6.

457 3.1.5. *Floating OWSCs*

458 Pictures of the floating OWSCs discussed in this section are shown in
459 figure 8.

460 • References [39] and [40] reports on experiments conducted on the Lan-
461 glee technology, consisting of oscillating flaps mounted on a floating
462 structure. Experiments were conducted at Aalborg University in Den-
463 mark. Experiments carried out at small scale in order to determine
464 the power performance of these devices in five random sea states with
465 significant height ranging from one to five meters. Mean annual CWR
466 were obtained by weighting power performance for each sea state with
467 its probability of occurrence at a site offshore Denmark. The mean an-
468 nual resource was 16 kW/m. Table 6 of source [39] shows that the
469 mean CWR was found to be 7 % for a device width 25 m and 9 % for
470 devices width 37.5 m and 50 m. Note that the total flap width has
471 been taken into account in the CWR. [40] reports on a second round of
472 experiments conducted on the same technology. The tested geometry

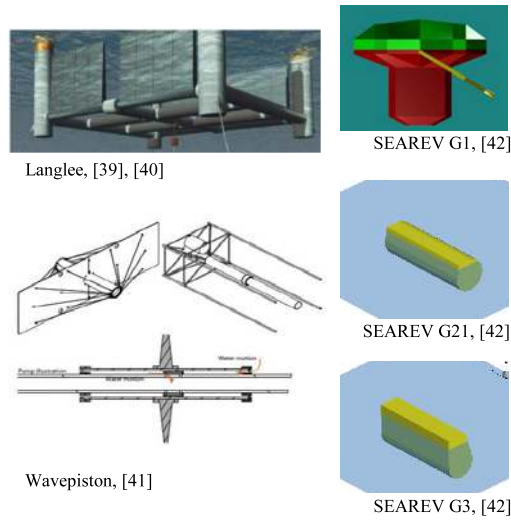


Figure 8: Pictures of the floating OWSCs covered by the sources reviewed in section 3.1.3.

473 differed from [39] in that: surface piercing flaps were used. This was
 474 found to increase efficiency compared to a fully submerged flap config-
 475 uration. Buoyancy of the flaps was also found to have a large impact
 476 on efficiency. Tables 3 and 4 of [40] show the estimates of yearly power
 477 production for several scales of the device (1/20, 1/40, 1/60) and two
 478 locations. For the Danish North Sea site, whose wave resource is 16
 479 kW/m, yearly power production is 620 MWh/y for a device width 25
 480 m. For the Runde site, whose wave resource is 21 kW/m, yearly power
 481 production is respectively 420 MWh/y, 1870 MWh/y and 3720 MWh/y
 482 for devices width 25 m, 50m and 100m. The total width of flaps for the
 483 device being twice the device width, the CWR is 9 % for the site with
 484 16 kW/m resource: for the site with 21 kW/m resource, the CWR is
 485 respectively 5 %, 10 % and 10% for devices width 25 m, 50 m and 100
 486 m.

- 487 • Reference [41] reports on experiments in Denmark using the Wavepis-
 488 ton technology. This device is made of vertical plates facing the waves
 489 and sliding along one long common axis, and can be classified as a
 490 variant of floating OWSC. As for references [9] and [39], the device was
 491 tested for five representative sea states. The mean CWR was obtained
 492 by weighting performance results by their probabilities, and mean CWR

493 is 8 % for a 15 m wide device (see table 3 of the paper) and a wave
494 resource of 12 kW/m. Another site offshore Italy was also considered,
495 for which mean CWR is 15 % for a wave resource of 3.5 kW/m.

496 • Reference [42] deals with the development of the SEAREV WEC tech-
497 nology. The SEAREV device absorbs wave power through pitch mo-
498 tion; as such, it can be classified as a variant of floating OWSC. Mean
499 annual absorbed power with and without control was derived using
500 numerical modeling. In the database, we retained only results with
501 passive control. Three versions of the SEAREV technology are pre-
502 sented in the source [42]. They are labelled SEAREV G1, SEAREV
503 G21 and SEAREV G3. The width of SEAREV G1 is 13.6 m, whereas
504 it is 30 m for SEAREV G21 and SEAREV G3. According to data
505 shown in tables 1, 2 and 5 of [42], the mean CWR are respectively 20
506 %, 16 % and 25 % for SEAREV G1, SEAREV G21 and SEAREV G3
507 for a site with 25 kW/m resource.

508 Power performance results for other floating OWSCs can be found in [11]
509 and [44]. These sources are discussed in section 3.1.6.

510 *3.1.6. Sources considering technologies with various working principles*

511 • Reference [43] is a report presenting results of a technical-economical
512 assessment of ten wave energy converters which were developed in the
513 UK in the late 70s and early 80s. Six of the devices are OWCs or
514 variants of OWCs, the others being variants of fixed OWSCs, including
515 the famous Edinburgh Duck and Bristol Cylinder. The devices are de-
516 picted in figure 9. Power performance was assessed using experiments
517 in directional random waves, except in the case of the NEL Termina-
518 tor device, for which numerical models were used. Scale models of the
519 devices were tested for 46 sea states representative of the South Uist
520 offshore site in the UK. Mean annual CWR for each technology are
521 shown in device data sheets in section 5 of source [43], and recalled in
522 table 2. It may be observed that power performance for the Vicker's
523 terminator, the Vicker's Attenuator and the Lancaster Flexible Bag is
524 significantly lower than for other devices with same operational prin-
525 ciple and comparable dimensions. According to [43], this is due to the
526 use of manifolding in the PTO.

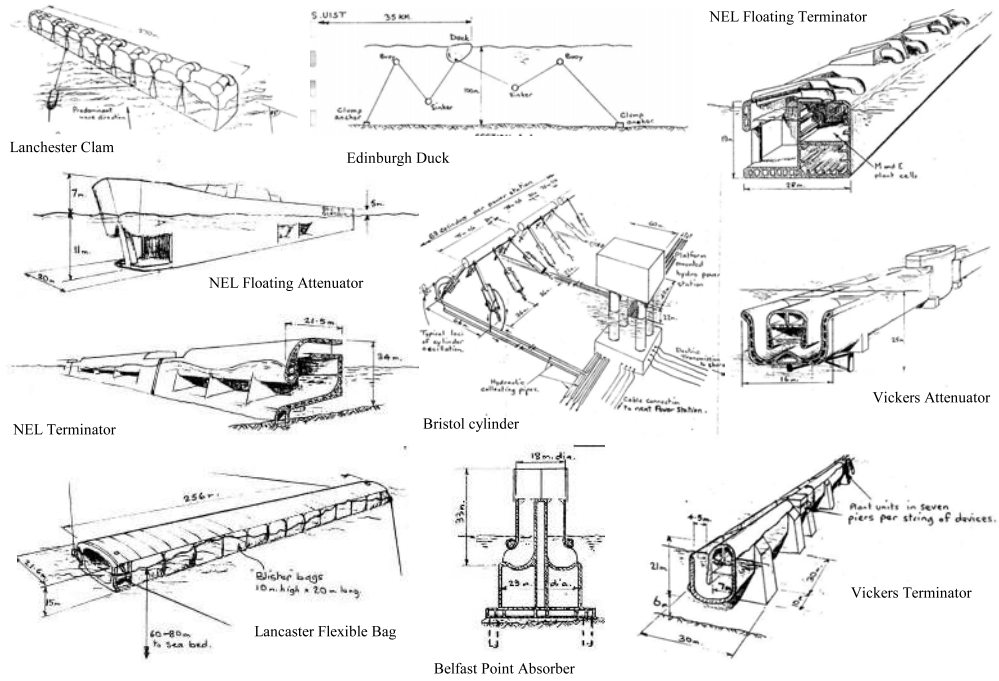


Figure 9: Pictures of wave energy converters investigated in [43].

Technology	operational principle	η_1	Dimension (m)		Resource (kW/m)
NEL Terminator	OWC	55	22	Width	30
NEL Floating Terminator	OWC	24	22	Width	54
NEL Floating Attenuator	OWC	41	20	Width	54
Vicker's Terminator	Variant of OWC	34	30	Width	36
Vicker's Attenuator	Variant of OWC	16	30	Width	36
Belfast Point Absorber	Variant of OWC	35	29	Outer diameter	42
Edinburgh Duck	Variant of OWSC	47	37	Width	54
Bristol Cylinder	Variant of OWSC	46	75	Width	48
Lancaster Flexible Bag	Variant of OWSC	9	20	Width	51
Lancaster Clam	Variant of OWSC	23	27	Width	51

Table 2: Performance results for technologies studied in [43]

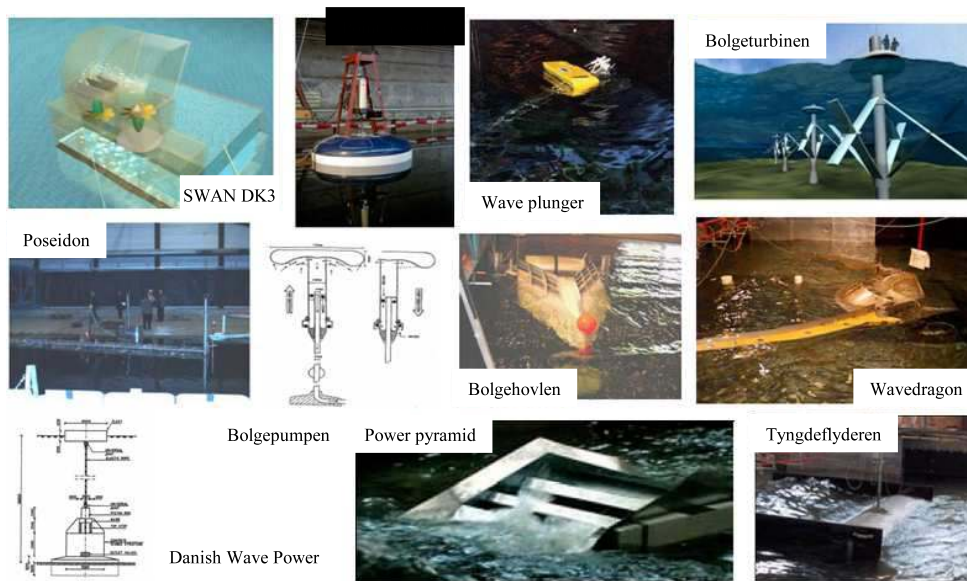


Figure 10: Pictures of wave energy converters investigated in [9].

- 527
- 528
- 529
- 530
- 531
- 532
- 533
- 534
- 535
- 536
- 537
- 538
- 539
- 540
- 541
- 542
- 543
- 544
- Reference [9] is the final report of a research program conducted in Denmark from 1997 to 2002. The aim of the program was to investigate a large number of WEC technologies. Twelve devices were considered: one floating OWC, several wave activated bodies, several overtopping devices and one wave turbine. The devices are depicted in figure 10. Experiments were conducted at small scale in order to determine the power performance of these devices in five random sea states with significant height ranging from one to five meters. Mean annual CWR were obtained by weighting power performance for each sea state with its probability of occurrence at a site offshore Denmark. The scatter diagram resulted from [56]. The mean annual resource was 16 kW/m. Mean annual CWR η_1 for each technology, directly taken from table 8.6 of source [9], is recalled in table 3. Note that for some cases, a few designs of the same technology were tested: in these cases, we retained only that with best performance. For heaving devices, we calculated the dimension using equation 4.
 - Reference [10] is a report presenting results from a study conducted by E2I EPRI on the technico-economical feasibility of wave energy conver-

Technology	operational principle	η_1	Dimension (m)		Resource (kW/m)
Swan DK3	OWC	20	16	Width	16
Bølgehovlen	Overtopping	8	10	Diameter	16
Power pyramid	Variant of overtopping	12	125	Width	16
Wavedragon	Overtopping	23	259	Width	16
Sucking Sea Shaft	Variant of overtopping	3	125	Width	16
Bølgepumpen	Variant of heaving device	6	5	Diameter	16
Point absorber	Heaving device	14	10	Diameter	16
DWP system	Heaving device	20	10	Diameter	16
Tyngdeflyderen	Variant of heaving device	12	30	Characteristic diameter	16
Wave plunger	Variant of fixed OWSC	16	15	Width	16
Poseidon	Unknown	27	420	Width	16
Bølgeturbinen	Wave turbine	4	15	Rotor diameter	16

Table 3: Performance results for technologies studied in [9]

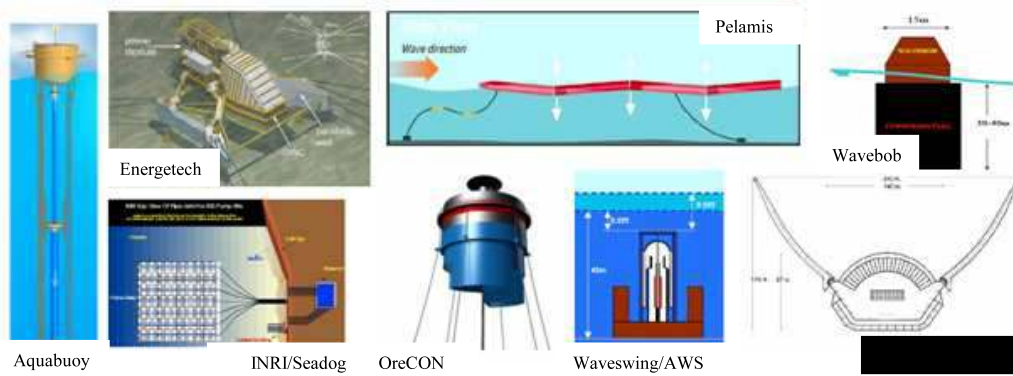


Figure 11: Pictures of wave energy converters investigated in [10].

Technology	operational principle	η_1	Dimension (m)		Resource (kW/m)
AquaEnergy/ AquaBuOY	heaving device	[10-26]	6	Diameter	[12-26]
Energetech	OWC	58	35	Width	[12-26]
INRI/SEADOG	heaving device	[16-24]	5.7	Diameter	[12-26]
Ocean Power Delivery/Pelamis	Variant of heaving device	[14-21]	15	Characteristic diameter	[12-26]
ORECON/ MR1000	OWC	[176-281]	32	Diameter	[12-26]
TeamWork/AWS	Variant of heaving device	[138-205]	9.5	Diameter	[12-26]
Wavebob	heaving device	[40-51]	15	Diameter	[12-26]
Wavedragon	overtopping	[21-26]	24	Width	[12-26]

Table 4: Performance results for technologies studied in [10]

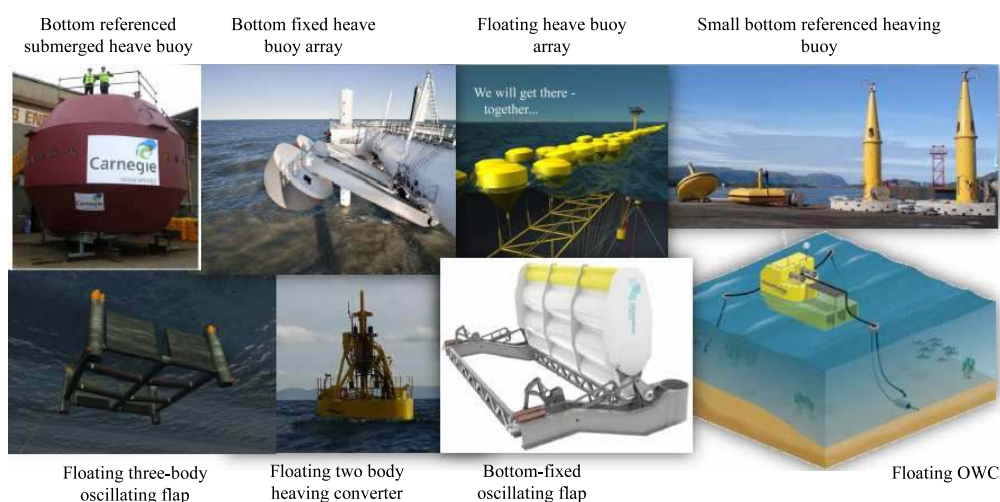


Figure 12: Pictures of wave energy converters investigated in [11].

545 sion in the US in 2004. Eight technologies were assessed: Ocean Power
546 Delivery (currently Pelamis Wave)/Pelamis, Energetech, Wavedragon,
547 Waveswing/AWS, Wavebob, Aquaenergy/AquaBuOY, OreCON and
548 INRI/SEADOG. The devices are depicted in figure 11. Power pro-
549 duction calculations were based on data and a power matrix provided
550 by the technology developers. Results have been extracted from the
551 report and summarized in table 4.

- 552 • Reference [11] presents the results of a numerical benchmarking study
553 of a selection of eight wave energy technologies inspired by devices
554 which are or were being developed. The selection includes a float-

Technology	operational principle	η_1	Dimension (m)		Resource (kW/m)
Small bottom-referenced heaving buoy	Variant of heaving device	[3-4]	3	Diameter	[15-37]
Bottom-referenced submerged heave-buoy	Heaving device	[8-13]	7	Diameter	[13-34]
Floating-two body heaving converter	Heaving device	[27-36]	20	Diameter	[15-37]
Bottom-fixed heave-buoy array	Heaving device	[12-17]	5	Diameter	[13-34]
Floating heave-buoy array	Heaving device	[6-11]	8	Diameter	[15-37]
Bottom-fixed oscillating flap	Fixed OWSC	[58-72]	26	Width	[13-34]
Floating three-body oscillating flap	Floating OWSC	[7-13]	19	Width	[15-37]
Floating OWC	OWC	[22-35]	24	Width	[15-37]

Table 5: Performance results for technologies studied in [11]

555 ing OWC, several heaving devices, one floating OWSC and one fixed
556 OWSC. The devices are shown in figure 12. The study used numerical
557 modeling: Wave to Wire (W2W) models were developed and used to
558 derive the power matrix of each technology. Then, the mean annual
559 power absorption was calculated at five European possible deployment
560 locations whose wave resource ranges from 15 to 80 kW/m. Depending
561 on the technology, it was shown that the mean CWR may depend sig-
562 nificantly on the resource, up to a factor of three. However, the lowest
563 mean CWR was always obtained for the most energetic site (80 kW/m
564 at Belmullet, Ireland). As this is much higher than the usual global fig-
565 ures for wave resource (10-40 kW/m, see [58]), we did not take it into
566 account. Table 5 summarizes mean CWR for the eight technologies
567 extracted from figures 12 to 19 of [11].

568 • [44] presents numerical results for the power performance of fixed and
569 floating OWSCs. Three configurations are considered : (A) one flap
570 mounted on a supporting frame, (B) two flaps that sit side by side and
571 (C) two flaps, one in the front and one in the back. The devices are
572 depicted in figure 13. In all configurations, the flap width is 25 m.
573 Numerical modeling was used to derive power matrices for each con-
574 figuration and for different mooring configurations (fixed supporting
575 frame, taut mooring and slack mooring). With the fixed supporting
576 frame, the devices are classified as variants of fixed OWSC because the
577 flap height is not close to the water depth. The wave scatter diagram
578 is shown in table 4. The wave resource is 30 kW/m. Annual average

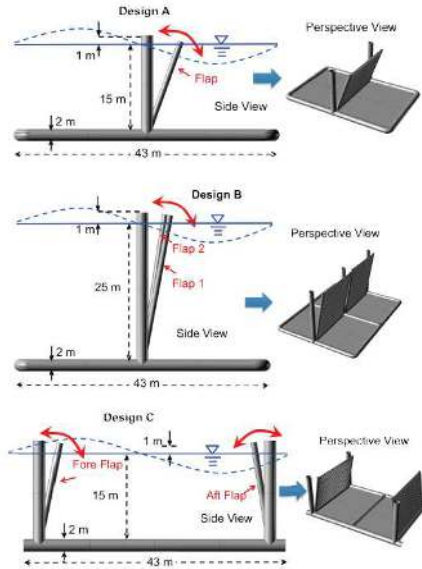


Figure 13: Pictures of wave energy converters investigated in [44].

579 electrical power is shown in figure 7 of the paper. 80 % PTO efficiency
 580 is assumed as well as 95 % availability and 98 % efficiency in the trans-
 581 mission line. Table 6 shows the mean annual absorbed power and CWR
 582 for the configurations considered in the paper.

- 583 • [45] presents numerical results for the power performance of a two-body
 584 heaving device and a fixed OWSC. The devices are shown in figure 14.
 585 The heaving device is 15 m wide. On page 99 of source [45], it is
 586 reported that the average electric power is 82 kW, with hydraulic PTO
 587 efficiency of 72 %. The wave resource at the site being 31 kW/m, the
 588 mean annual CWR is 25 %. For the fixed OWSC, the width is 25.5 m.
 589 It is reported (page 108 of source [45] that the average electric power
 590 is 170 kW with hydraulic PTO efficiency of 75 %. The wave resource
 591 at the site being 18 kW/m, the mean annual CWR is 49 %.

592 3.2. Summary table

593 The data collected for mean annual CWR is synthesized in tables 7, 8 and
 594 9. The WECs have been grouped in ten categories as discussed in section 2.3:

Technology	operational principle	Mean absorbed power per flap	η_1	Dimension (m)		Resource (kW/m)
Vertical flaps on fixed supporting frame	Variant of fixed OWSC	240	31	25	Width	30
		450	37	50		
		220	30	25		
Vertical flaps on supporting frame with taut moorings	Floating OWSC	138	18	25	Width	30
		266	18	50		
Vertical flaps on supporting frame with slack moorings	Floating OWSC	58	8	25	Width	30
		128	8	50		
		158	21	25		

Table 6: Performance results for technologies studied in [44]

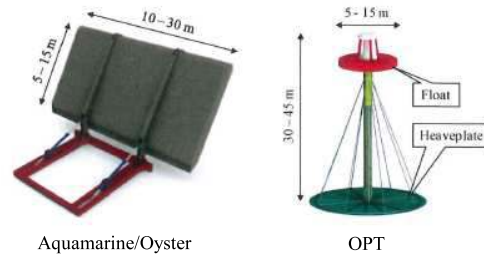


Figure 14: Pictures of wave energy converters investigated in [45].

595 OWCs and variants, overtopping devices and variants, heaving devices and
596 variants, fixed OWSC and variants, floating OWSC and variants. Devices
597 not belonging to any of these categories were not included in the tables. In
598 these, the devices are labeled by their commercial names when available, or
599 by the description of their operational principle. CWR is reported alongside
600 the corresponding wave resource for which it was measured and the dimension
601 on which the CWR was built.

602 Where available, information relating to how the CWR was obtained
603 (model tests, numerical modeling or measurements on full scale prototype)
604 is also reported. In more than half of the cases, CWR were obtained through
605 experiments at model scale or prototype scale.

606 The tables also indicate whether the source is independent from the tech-
607 nology developer. 'Developer' indicates that the information comes from the
608 technology developer itself whereas 'independent' means that the CWR was
609 established by an independent body (usually a research lab).

610 4. Discussion

611 In total, 156 measurements of CWR were collected. Figure 15 shows
612 the distribution of measurements as a function of the WEC categories. The
613 category for which the most performance information was found (56 mea-
614 surements) was heaving devices, followed by fixed OWSCs and OWCs. This
615 is somewhat surprising, as OWCs have been studied for more than 30 years,
616 whereas fixed OWSCs have only started developing over the last decade. The
617 least information was found for floating OWSCs and overtopping devices.

618 Some of the measurements are believed to be unreliable (lines in italics
619 in tables 7 and 8). Indeed, for the AWS and the ORECON/MR1000, the
620 CWR is five to ten times larger than other similar technologies. Because
621 the available source information does not provide an explanation for these
622 discrepancies, these measurements were discarded from further analysis. The
623 Hydrocap/SEACAP device was also discarded because it is five times smaller
624 than device of similar dimensions, and because as explained before, the per-
625 formance is small because the PTO damping coefficient was optimized for
626 the resonant period in regular waves, and not for the mean annual power
627 absorption in irregular waves.

628 Moreover, for some of the technologies, CWR is available for several levels
629 of wave resource. The CWR for the level of wave resource closest to 25 kW/m
630 was selected as the most representative [58].

Category	Technology	η_1 (%)	Resource (kW/m)	Characteristic dimension(m)		Ref.	Methods	Source	
Oscillating Water Column	NEL Terminator	55	30	22	Width	[43]	Model tests	Independent	
	NEL Floating Terminator	24	54	22	Width	[43]	Model tests	Independent	
	NEL Floating Attenuator	41	54	20	Width	[43]	Model tests	Independent	
	Swan DK3	20	16	16	Width	[9]	Model tests	Independent	
	Energetech		72	12	35	Width	[10]	N/A	Developer
			58	21					
			58	26					
	ORECON/ MR1000		33	15	32	Diameter	[10]	N/A	Developer
			213	12					
			209	21					
			176	26					
	Floating OWC		281	15	24	Width	[11]	N/A	Independent
			23	15					
			32	22					
			35	27					
NEL-OWC		24	37	30	Width	[14]	Sea trials	Developer	
		22	16						
		27	23						
Mutriku wave power plant		29	27	6	Width	[15]	Model tests	Developer	
		23	37						
Pico		7	26	12	Width	[17]	Prototype	Independent	
Variant of oscillating water column	Vickers Terminator	20	38	30	Width	[43]	Model tests	Independent	
	Vickers Attenuator	34	36	30	Width	[43]	Model tests	Independent	
	Belfast Point absorber	16	36	29	Diameter	[43]	Model tests	Independent	
	Floating OWC		35	42	8	Diameter	[16]	Numerical modelling	Independent
			17	31					
	KNSWING		23	14	7.5	Width	[18]	Model tests	Developer
	Floating OWC		12	15	12.5	Width	[19]	Model tests	Independent
14			23						
		15	27						
		12	36						
Overtopping devices	Bolgehovlen	8	16	10	Diameter	[9]	Model tests	Independent	
	Wavedragon		23	16	259	Width	[9]	Model tests	Independent
			26	12					
	Wavedragon		23	21	300	Width	[10]	N/A	Developer
			21	26					
22			15						
Wavedragon		27	6	65	Width	[21]	Model tests	Developer	
		18	97						
Variant of overtopping devices	Power pyramid	12	16	125	Width	[9]	Model tests	Independent	
	Sucking Sea Shaft	3	16	125	Width	[9]	Model tests	Independent	
	SSG	23	19.5	10	Width	[20]	Model tests	Developer	

Table 7: Summary table of energy performance of wave energy converters

Category	Technology	η_1 (%)	Resource (kW/m)	Characteristic dimension(m)	Ref.	Methods	Source		
Heaving devices	Point absorber	14	16	125	Width	[9]	Model tests	Independent	
	DWP system	20	16	10	Diameter	[9]	Model tests	Independent	
	AquaEnergy/ AquaBuOY		20	12	6	Diameter	[10]	N/A	Developer
			17	21					
			14	26					
			21	15					
	INRI/SEADOG		24	12	5.7	Diameter	[10]	N/A	Developer
			16	21					
			16	26					
	Wavebob		21	15	15	Diameter	[10]	N/A	Developer
			40	12					
			51	21					
			46	26					
	Small bottom-referenced heaving buoy		4	15	3	Diameter	[11]	Numerical modelling	Independent
			4	22					
			4	27					
			3	37					
	Floating two-body heaving converter		27	15	20	Diameter	[11]	Numerical modelling	Independent
			29	22					
			36	27					
			27	37					
	Bottom-fixed heave-buoy array		14	13	5	Diameter	[11]	Numerical modelling	Independent
			16	19					
			17	22					
			12	34					
	Floating heave-buoy array		11	15	8	Diameter	[11]	Numerical modelling	Independent
			11	22					
		11	27						
		6	37						
Two-body heaving device	25	31	15	Diameter	[45]	Numerical modelling	Independent		
<i>Hydrocap/ SEACAP</i>		4		10	<i>Diameter</i>	<i>[22]</i>	<i>Numerical modelling</i>	<i>Independent</i>	
		3		11					
		6	25	15					
		6		16.5					
		9		20					
Inspired by OPT	19	40	10	Diameter	[23]	Numerical modelling	Independent		
LifeSaver	12.5	27	12.5	Diameter	[25]	Prototype	Developer		
Inspired by Wavestar		10	N/A	4	Diameter	[26]	Numerical modelling	Independent	
		15		15					
Lifesaver	12	26	12.5	Characteristic diameter	[25]	Prototype	Developer		
RM3	16	34	20	Diameter	[27]	Numerical modelling	Independent		
Variant of heaving devices	Bolgepumpen	6	16	5	Diameter	[9]	Model tests	Independent	
	Tyngdeflyderen	12	16	30	Characteristics diameter	[9]	Model tests	Independent	
	Pelamis		21	12	15	Characteristic diameter	[10]	N/A	Developer
			15	21					
			14	26					
	AWS		18	15	9.5	<i>Diameter</i>	<i>[10]</i>	<i>N/A</i>	<i>Developer</i>
			138	12					
			205	21					
			142	26					
	Bottom-referenced submerged heave-buoy		145	15	7	Diameter	[11]	Numerical modelling	Independent
			9	13					
		13	19						
DEXA		13	22	31	Characteristic diameter	[24]	Model tests	Independent	
		8	34						
		8	26	22					

Table 8: Summary table of energy performance of wave energy converters (continued)

Category	Technology	η_1 (%)	Resource (kW/m)	Characteristic dimension(m)		Ref.	Methods	Source	
Fixed OWSC	Bottom-fixed oscillating flap	61	13	26	Width	[11]	Numerical modelling	Independent	
		68	19						
		72	22						
		58	34						
	Bottom-fixed oscillating flap	49	18	25.5	Width	[45]	Numerical modelling	Independent	
	Biopower	45	38.5	6.6	Diameter	[30]	Model tests	Developer	
	OWSC		35	N/A		Width	[31]	Model tests	Developer
			52						
			65						
	Inspired by Oyster		22	26		Width	[35]	Numerical modelling	Independent
			40						
			55						
Surface piercing flap		17	26		Width	[38]	Numerical modelling	Independent	
		36							
		72							
		64							
Variant of fixed OWSC	Edinburgh Duck	47	54	37	Width	[43]	Model tests	Independent	
	Bristol Cylinder	46	48	75	Width	[43]	Model tests	Independent	
	Lancaster flexible bag	9	51	20	Width	[43]	Model tests	Independent	
	Lanchester Clam	23	51	27	Width	[43]	Model tests	Independent	
	Wave plunger	16	16	15	Width	[9]	Model tests	Independent	
	Vertical flaps on fixed supporting frame		31	25	30	Width of each flap	[44]	Numerical modelling	Independent
			37						
			30						
	Top-hinged flaps	25	25	12	Width	[29]	Model tests	Independent	
	WEPTOS		10	16	2.9	Width	[32], [33], [34]	Model tests	Independent
			12						
			15						
			15						
			19						
			32						
25									
26									
9.6									
Combined wind and wave energy platform	45	26	16	Width	[36]	Numerical modelling	Independent		
Combined wind and wave energy platform	61	26	9	Width	[37]	Numerical modelling	Independent		
Floating OWSC	Floating three-body oscillating flap	9	15	19	Width	[11]	Numerical modelling	Independent	
		13							
		13							
		7							
	Vertical flaps on supporting frame with taut moorings		18	25	30	Width	[44]	Numerical modelling	Independent
			18						
	Vertical flaps on supporting frame with slack moorings		8	25	30	Width	[44]	Numerical modelling	Independent
			8						
	21	25							
	Langlee		7	16	25	Width	[39],[40]	Model tests	Independent
5									
9									
9									
10	16	37.5							
10	21	50							
10	21	50							
10	21	100							
Variant of floating OWSC	Wavepiston	15	12	32	15	[41]	Model tests	Independent	
		8	3.5						
	SEAREV G1	20							13.6
	SEAREV G21	16	25						30
SEAREV G3	25		30						

Table 9: Summary table of energy performance of wave energy converters (continued)

		OWCs	Overtopping devices	Heaving devices	Fixed OWSCs	Floating OWSCs
Capture width ratio (%)	Mean	29	17	16	37	12
	STD	13	8	10	20	5
Characteristic dimension (m)	Mean	20	124	12	18	33
	STD	10	107	7	14	24

Table 10: Mean and standard deviation of CWR and characteristic dimension for each WEC category

631 After screening, 90 measurements were retained for further analysis. The
632 two categories with the most measurements in the screened data, including
633 variants, are fixed OWSCs and heaving devices, with 30 and 24 measurements
634 respectively. OWCs, floating OWSCs and overtopping devices had 16, 12
635 and 8 measurements, respectively. Excluding variants, the categories with
636 most measurements are heaving devices and fixed OWSCs, both with 14
637 measurements. OWCs, floating OWSCs and overtopping devices had 9, 8
638 and 5 measurements, respectively.

639 Statistical analysis was performed. For each category, table 10 shows the
640 mean and the standard deviation for both the CWR and the characteristic
641 dimension of the WECs. Variants were taken into account. According to
642 the mean, the most efficient category of WECs is fixed OWSCs with a mean
643 CWR of 37 %. The second most efficient WECs are OWCs (mean CWR of
644 29%), followed by overtopping devices (17 %), heaving devices (16 %) and
645 floating OWSCs (12 %).

646 One can see that standard deviations of the CWR are large - typically,
647 half of the mean CWR. This shows that, within a given category, the power
648 performance of devices can differ widely. However, the mean CWR gives a
649 good indication of the typical order of magnitude of the power performance
650 of each of these categories.

651 From table 10, it can also be seen that heaving devices are typically the
652 smallest WECs (having mean characteristic dimension 12 m). The second
653 smallest are the fixed OWSCs (18m) and the OWCs (20m), followed by the
654 floating OWSCs (33m) and the large overtopping devices (124m).

655 Figure 16 shows the CWR as a function of the WEC characteristic di-
656 mension and the WEC category. Although the level of scattering is large,
657 trends can be identified:

- 658 • Floating OWSCs and overtopping devices appear to be the least effi-
659 cient devices, in terms of absorbing wave energy.

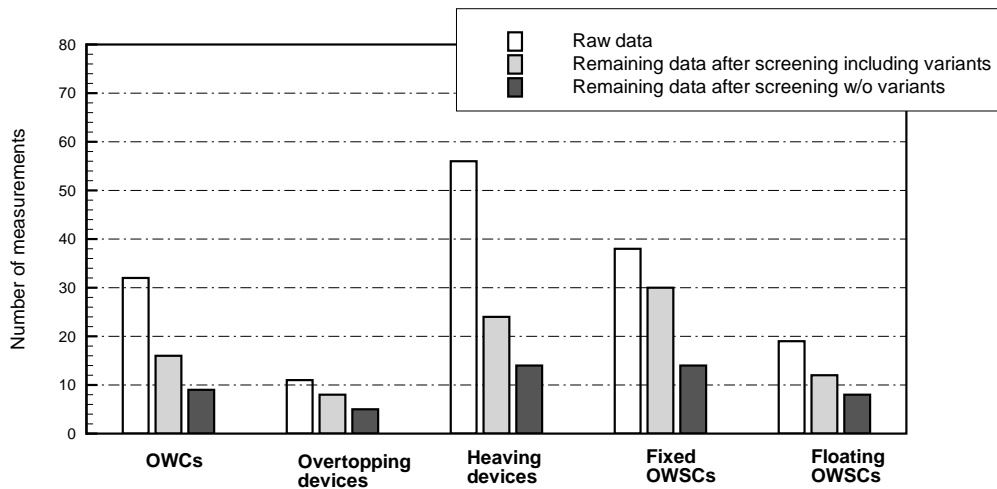


Figure 15: Number of measurements per category of WECs.

- 660 • Fixed OWSCs appear to be the most efficient devices.
- 661 • Heaving devices and OWCs appear to be in the middle of the efficiency
- 662 range.

663 Being able to identify these trends from the data gives confidence in the
 664 classification that has been used (OWCs, overtopping devices, heaving de-
 665 vices, fixed and floating OWSCs). It indicates that the classification reflects
 666 rather well the underlying physical principles that lead to wave energy ab-
 667 sorption by these WEC technologies.

668 It can be seen from figure 16 that CWR increases with the characteristic
 669 dimension for OWCs, heaving devices, overtopping devices and fixed OWSCs.
 670 Linear regression was performed for these categories on the most representa-
 671 tive measurements points (i.e variants were not taken into account).

672 It yields a reasonable fit for the OWCs and the heaving devices, the
 673 coefficient of determination being 0.57 for the OWCs and 0.42 for the heaving
 674 devices. For overtopping devices, the linear fit is only approximate, the
 675 coefficient of determination being 0.21. This is due to the limited number
 676 of measurement points and an outlier having high CWR (27 %) for the
 677 width of 65 m. One may note that the wave resource corresponding to this
 678 measurement point is much smaller (6kW/m) than for the other measurement

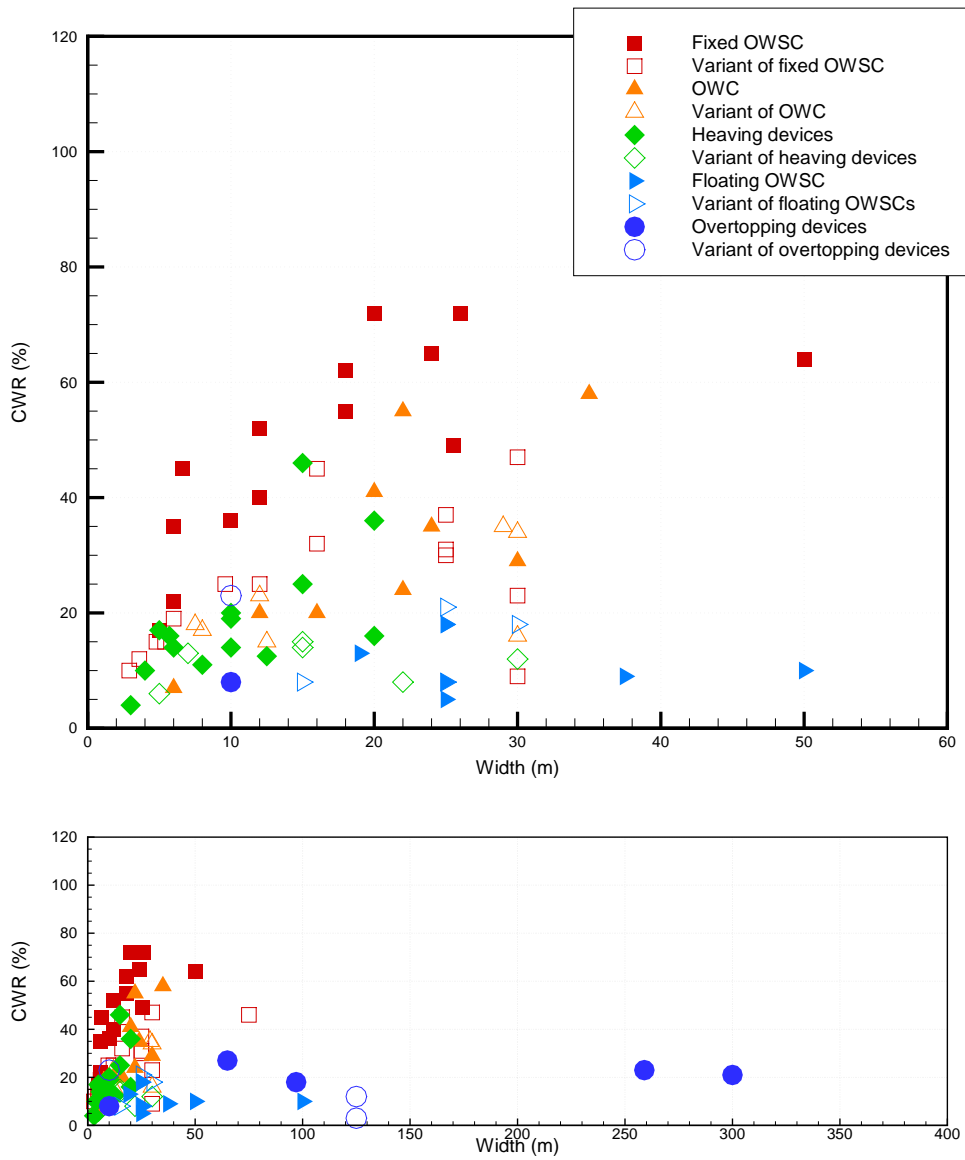


Figure 16: CWR as a function of the WEC characteristic dimension and the WEC category. Top figure zooms in on the subdomain $[0,60]$ m part of the bottom figure.

	Best fit	95 % confidence interval
OWCs	$\tilde{\eta}_1 = 1.4B + 2.1, B \in [0, 40]$	$\tilde{\eta}_1 \pm 30\sqrt{1.1 + \frac{(B-21)^2}{81}}$
Overtopping devices	$\tilde{\eta}_1 = 0.026B + 15.6, B \in [0, 320]$	$\tilde{\eta}_1 \pm 26\sqrt{1.2 + \frac{(B-146)^2}{7230}}$
Heaving devices	$\tilde{\eta}_1 = 1.3B + 5.6, B \in [0, 20]$	$\tilde{\eta}_1 \pm 21\sqrt{1.1 + \frac{(B-10)^2}{31}}$
Fixed OWSCs	$\tilde{\eta}_1 = 1.9B + 20.5, B \in [0, 20]$	$\tilde{\eta}_1 \pm 25\sqrt{1.1 + \frac{(B-15)^2}{61}}$
Floating OWSCs	$\tilde{\eta}_1 = 8.5, B \in [0, 100]$	$\tilde{\eta}_1 \pm 12\sqrt{1.1 + \frac{(B-53)^2}{1090}}$

Table 11: Best fit equations and 95% confidence interval for each WEC category

679 points (in the order of 20 kW/m, see table 7). It may be expected that the
680 same device at a site with larger wave resource has a smaller CWR, thus
681 more in agreement with the linear fit.

682 For fixed OWSCs, it can be observed in 16 that CWR increases with
683 width for widths between 0 up to 30 m. In the database 9, it can be seen
684 that several devices in this category have a CWR greater than 50 % for
685 widths in the order of 20 to 30 m. On the other hand, it is well known from
686 [50] that the maximum CWR is 50 % for devices whose width is greater than
687 the wavelength. Consequently, the increase in CWR with width that can
688 be seen in figure 16 for fixed OWSCs must be valid only for small widths.
689 When further increasing the width, the CWR must reach a maximum and
690 then decrease below 50 % for long devices. This is in agreement with the
691 outlier with width 50 m, whose CWR is smaller than similar devices with
692 half its width. Thus, linear fit was performed only on measurements points
693 with width less than 30 m for fixed OWSCs. It yields a reasonable fit, the
694 coefficient of determination being 0.69.

695 For floating OWSCs, there is no clear relationship between the CWR and
696 the characteristic dimension. For these categories, the best fit appears to be
697 the mean value of the data.

698 For each category, table 11 shows the best fit equations and the 95%
699 confidence interval, calculated according to [57]. Figure 17 shows, for each
700 category, the data points, the best fit equations and the 95% confidence
701 interval. One can see that all data points are covered by the confidence
702 interval. For each category, devices which are variants of the operational
703 principle have also been plotted (empty symbols). Again, all these points
704 except one are covered by the confidence interval. This gives confidence in
705 the classification choices that have been made in this work.

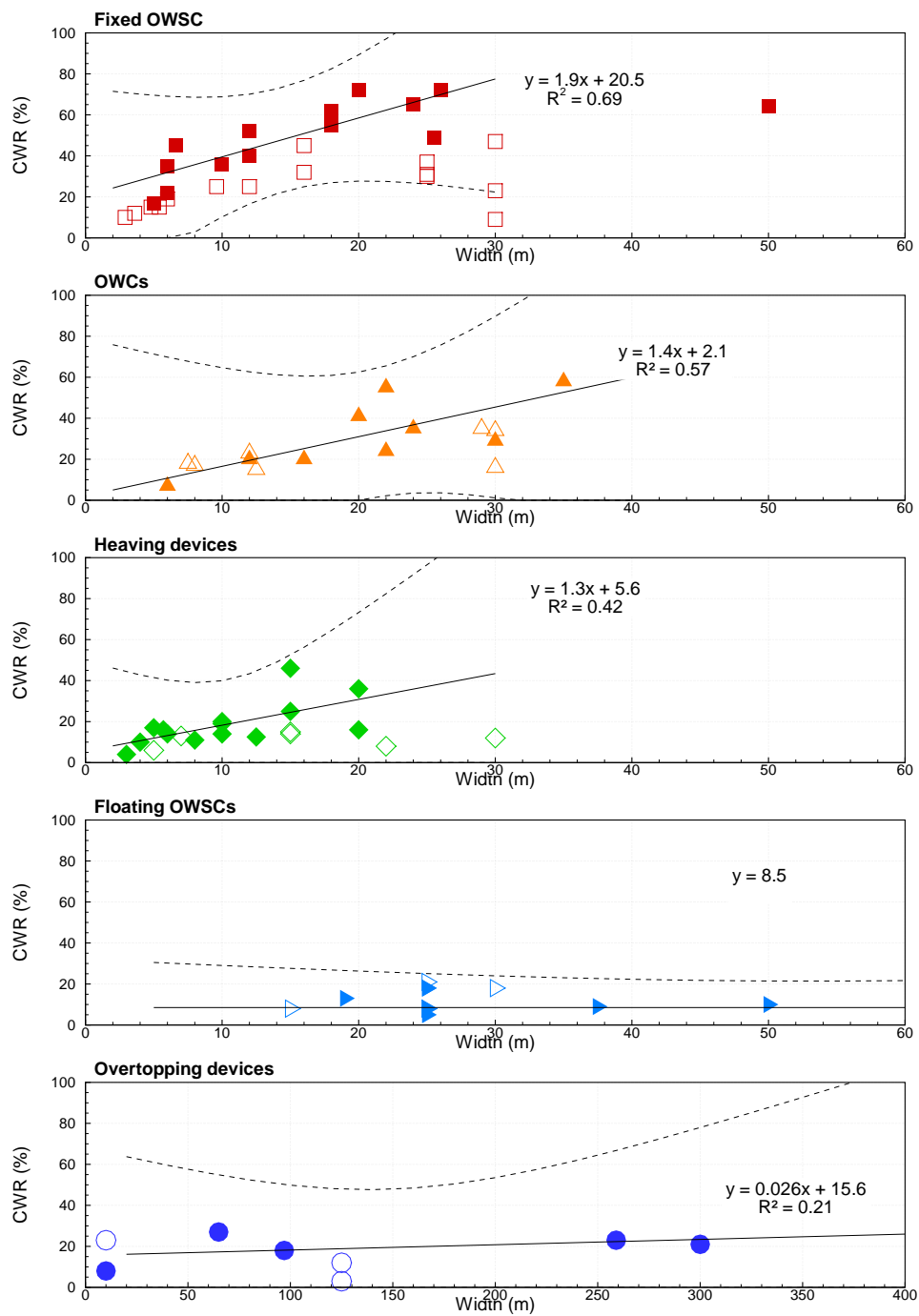


Figure 17: Data points, best fit equations and 95 % confidence interval for each category of WECs. For each category, empty symbols are for devices which are variants of the archetypal realization.

706 Conversely, the results from the statistical analysis (table 11) may be used
707 to estimate the typical power performance for a given category of WEC, a
708 characteristic dimension B and a for given mean wave resource J using:

$$P = \tilde{\eta}_1 B J \quad (5)$$

709 This may be useful in the early stages of WEC design, in order to check
710 whether power performance of a particular WEC is in the range of perfor-
711 mance figures available in the literature. It may help in detecting mistakes in
712 the early stage of modelling, for instance, and may also be used in technico-
713 economical prospective studies in order to estimate the wave energy potential
714 of typical WEC technologies. However, it should not be used to assess the
715 actual performance of a given WEC as it may differ significantly from the
716 typical power performance of WECs of the considered category.

717 5. Conclusion

718 In this paper, available information from the literature relating to hydro-
719 dynamic power performance of WECs has been reviewed. A database was
720 established that contains information on the WEC category (OWCs, over-
721 topping devices, heaving devices, fixed OWSCs, floating OWSCs), its CWR,
722 its characteristic dimension, the wave resource, the methodology that was
723 used to derive the performance, and the reference for the information.

724 Analysis of this database indicated that the least efficient categories of
725 WECs, in terms of absorbing wave energy, are floating OWSCs and over-
726 topping devices, the most efficient are fixed OWSCs, with heaving devices
727 and OWCs in the middle of the efficiency range. It is important to note
728 that here, efficiency relates to hydrodynamic power performance (energy ab-
729 sorption) and not economical performance (cost of energy). Efficiency in the
730 PTO system and the power conversion chain, as well as fabrication and op-
731 eration costs, may be such that the most efficient device hydrodynamically
732 speaking can be the least efficient device from perspective of cost of energy.

733 Statistical analysis was performed and statistical relationships were de-
734 rived relating CWR to the characteristic dimension of WECs and the WEC
735 category. It must be noted that uncertainties are large in the statistical re-
736 sults, as the number of measurements is rather small. However, it is believed
737 that this statistical work may prove to be useful both in high level prospective
738 studies and in detecting mistakes in the early stages of modeling.

739 It was observed that hydrodynamic performance varies significantly de-
740 pending on the WEC category. In order to further investigate the underlying
741 reasons for this, future work may compare capture width as a function of an-
742 gular frequency for typical examples of the categories. Finally, WECs not
743 belonging to one of the five categories listed above were not considered in
744 this study because they are relatively new concepts and would constitute a
745 category of their own. When more information becomes available for these
746 new technologies, it may be interesting to compare their hydrodynamic per-
747 formance with those of the categories considered in this paper.

748 **6. Acknowledgements**

749 The author gratefully acknowledges the financial support of the French
750 Institut pour la Transition Energetique (ITE) France Energies Marines.

751 **7. References**

- 752 [1] J. Falnes (2007) A review of wave energy extraction. *Marine Structures*,
753 Vol. 20, pp. 185-201
- 754 [2] B. Drew, A.R. Plummer, M.N. Sahinkaya (2009) A review of wave energy
755 converter technology. *Proc. ImechE Vol. 223 Part A: Journal of Power
756 and Energy*, pp. 887-902
- 757 [3] R. Sabzehgar, M. Moallem (2009) A review of ocean wave energy con-
758 version systems. In *Proc. of the 2009 IEEE Electrical Power & Energy
759 Conference*, Montreal, QC, Canada
- 760 [4] A. F. de O. Falcão (2010) Wave energy utilization: a review of tech-
761 nologies. *Renewable and Sustainable Energy Reviews*, Vol 14(3), pp.
762 889-918
- 763 [5] J. Aubry, H. Ben Ahmed, B. Multon, A. Babarit, A.H. Clement (2011)
764 Wave energy converters. In *Marine Renewable Energy Handbook*, Mul-
765 ton (Ed), Wiley-ISTE, Paris, pp. 323-363
- 766 [6] C. Guedes Soares, J. Bhattacharjee, M. Tello, L. Pietra (2012) Review
767 and classification of wave energy converters. In *Maritime Engineering
768 and Technology*, Guedes Soares et al. (Eds), Taylor & Francis Group,
769 London, pp. 85-594

- 770 [7] I. Lopez, J. Andreu, S. Ceballos, I. Martinez de Alegria, I. Kortabarria
771 (2013) Review of wave energy technologies and the necessary power-
772 equipment. *Renewable and Sustainable Energy Reviews*, Vol. 27, pp.
773 413-434
- 774 [8] C. Guedes Soares, J. Bhattacharjee, D. Karmakar (2014) Overview and
775 prospects for offshore wave and wind energy. *Brodogradnja*, Vol. 65(2),
776 pp. 91-113
- 777 [9] N.I. Meyer, M. McDonald Arnskov, L.C.E. Vad Bennetzen, H.F. Bur-
778 charth, J. Bungler, V. Jacobsen, P. Maegaard, S. Vindelov, K. Nielsen,
779 J.N. Sørensen (2002) Bølgekraftprogram: Afsluttende rapport fra En-
780 ergistyrelsens Rådgivende Bølgekraftudval Bølgekraftudvalgets Sekre-
781 tariat, Rambøll, Teknikerbyen 31, 2830 Virum, Denmark. *In Danish*
- 782 [10] M. Previsic, R. Bedard, G. Hagerman (2004) E2I EPRI Assessment:
783 Offshore Wave Energy Conversion Devices, E2I EPRI WP-004-US-Rev1,
784 Electricity Innovation Institute
- 785 [11] A. Babarit, J. Hals, M.J. Muliawan, A. Kurniawan, T. Moan, J.
786 Krokstad (2012) Numerical benchmarking study of a selection of wave
787 energy converters. *Renewable Energy*, Vol 43, pp. 44-63 (with Corrigendum
788 in *Renewable Energy*, 2015, Vol. 74, pp. 955-957)
- 789 [12] A. Pecher (2012) Performance evaluation of wave energy converters. Aal-
790 borg: Department of Civil Engineering, Aalborg University. (DCE Thesis;
791 No. 38)
- 792 [13] A. Babarit, J. Hals (2011) On the maximum and actual capture width
793 ratio of wave energy converters. In *Proc. of the 11th European Wave
794 and Tidal Energy Conference*, Southampton, UK
- 795 [14] B.M. Count (1982) On the hydrodynamic characteristics of wave en-
796 ergy absorption. In *Proc. of the 2nd International Symposium on Wave
797 energy utilization*, Trondheim, Norway, pp. 155-174
- 798 [15] Y. Torre-Enciso, I. Ortubia, L.I. Lopez de Aguilera, J. Marques (2009)
799 Mutriku Wave Power Plant: from the thinking out to the reality. In
800 *Proc. Of the 8th European Wave and Tidal Energy Conference*, Uppsala,
801 Sweden

- 802 [16] R.P.F. Gomes, J.C.C. Henriques, L.M.C. Gato, A.F.O. Falcão (2011)
803 Design of a Floating Oscillating Water Column for Wave Energy Conver-
804 sion, in Proc. Of the 9th European Wave and Tidal Energy Conference,
805 Southampton, UK
- 806 [17] A. Pecher, I. Le Crom, J.P. Kofoed, F. Neumann, E. de Brito Azevedo
807 (2011) Performance assessment of the Pico OWC power plant following
808 the EquiMar methodology, in Proc. Of the 21th International Offshore
809 and Polar Engineering Conference, Hawaii, USA
- 810 [18] K. Nielsen, F. P. Jacobsen, M. Simonsen, P. Scheijgrond (2013) Atten-
811 tuator development phase I, MARINET Infrastructure Access Report,
812 Infrastructure: UCC-HMRC Ocean Wave Basin, User-Project: KN-
813 SWING, MARINET-TA1-KNSWING
- 814 [19] T. Kelly, T. Dooley, J. Campbell, J. Ringwood (2013) Comparison of the
815 experimental and numerical results of modelling a 32-oscillating water
816 column (OWC), V-Shaped floating wave energy converters. *Energies*,
817 Vol. 6, pp. 4045-4077
- 818 [20] L. Margheritini, D. Vicinanza, P. Frigaard (2009) SSG wave energy con-
819 verter: Design, reliability and hydraulic performance of an innovative
820 overtopping device. *Renewable Energy*, Vol. 34, pp. 1371-1380
- 821 [21] S. Parmeggiani, J.F. Chozas, A. Pecher, E. Friis-Madsen, H.C. Sorensen,
822 J.P. Kofoed (2011) Performance assessment of the Wave Dragon wave
823 energy converter based on the Equimar methodology. In Proc. Of the
824 9th European Wave and Tidal Energy Conference, Southampton, UK
- 825 [22] V. Baudry, A. Babarit (2010) Assessment of the annual energy produc-
826 tion of a heaving wave energy converter sliding on the mast of a fixed
827 offshore wind turbine, in Proc. of the World Renewable Energy Congress
828 XI
- 829 [23] J.A. Oskamp, H.Y. Ozkan-Haller (2012) Power Calculations for a Pas-
830 sively Tuned Point Absorber Wave Energy Converter on the Oregon
831 Coast, *Renewable Energy*, Vol. 42, pp. 72-77
- 832 [24] B. Zanuttigh, E. Angelelli, J.P. Kofoed (2013) Effects of mooring sys-
833 tems on the performance of a wave activated body energy converter,
834 *Renewable Energy*, Vol. 57, pp. 422-431

- 835 [25] J. Sjolte, I.K. Bjerke, G. Tjensvoll, M. Molinas (2013) Summary of per-
836 formance after one year of operation with the Lifesaver Wave Energy
837 Converter System. In Proc. Of the 10th European Wave and Tidal En-
838 ergy Conference, Aalborg, Denmark
- 839 [26] A.D. de Andrés, R. Guanache, C. Vidal, I.J. Losada (2014) Analysis
840 of the geometric tunability of a WEC from a worldwide perspective.
841 In Proc. Of the 33rd International Conference on Ocean, Offshore and
842 Artic Engineering, San Francisco, California, USA
- 843 [27] V. Neary, M. Previsic, R.A. Jepsen, M.J. Lawson, Yi-Hsiang Yu, A.E.
844 Copping, A.A. Fontaine, K.C. Hallet D.K. Murray (2014) Method-
845 ology for design and economic analysis of marine energy conversion
846 (MEC) technologies. Technical report from Sandia National Laborato-
847 ries (USA), SAND2014-9040
- 848 [28] D. Skyner (1987) Solo Duck Linear Analysis, Technical Report, Univer-
849 sity of Edinburgh
- 850 [29] M. Folley, T.J..T. Whittaker, A. Henry (2007) The effect of water depth
851 on the performance of a small surging wave energy converter. Ocean
852 Engineering, Vol. 34, pp. 1265-1274
- 853 [30] F. Flocard, T.D. Finnigan (2009) Experimental investigation of power
854 capture from pitching point absorbers. In Proc. 8th European Wave and
855 Tidal Energy Conference, Uppsala, Sweden
- 856 [31] A. Henry, K. Doherty, L. Cameron, T. Whittaker, R. Doherty (2010)
857 Advances in the design of the Oyster wave energy converter, In Proc.
858 Royal Institution of Naval Architects Marine and Offshore Renewable
859 Energy Conference
- 860 [32] A. Pecher, J.P. Kofoed, T. Larsen (2012) Design Specifications for the
861 WEPTOS Hansthom WEC, Energies, Vol. 5(4), pp. 1001-1017
- 862 [33] A. Pecher, J.P. Kofoed, T. Larsen, T. Marchalot (2012) Experimental
863 study of the WEPTOS wave energy converter. In Proc. Of the 21th
864 International Conference on Ocean, Offshore and Artic Engineering, Rio
865 de Janeiro, Brazil

- 866 [34] A. Pecher, J.P. Kofoed, T. Larsen (2014) The extensive R&D behind
867 the Weptos WEC. In Proceedings of the 1st International Conference
868 on Renewable Energies Offshore (RENEW2014), Lisbon, Portugal
- 869 [35] E. Renzi, F. Dias (2012) Resonant behaviour of an oscillating wave en-
870 ergy converter in a channel, *Journal of Fluid Mechanics*, Vol. 701, pp.
871 482-510
- 872 [36] T. Soulard, A. Babarit, B. Borgarino (2012) Estimation de la production
873 d'une plateforme flottante hybride pour la récupération de l'énergie des
874 vagues et du vent. In Proc. of the 13emes Journees de l'hydrodynamique,
875 Chatou, France
- 876 [37] T. Soulard, A. Babarit, B. Borgarino (2013) Preliminary assessment of a
877 semi-submersible floating wind turbine combined with pitching wave en-
878 ergy converters. In Proc. Of the 10th European Wave and Tidal Energy
879 Conference, Aalborg, Denmark
- 880 [38] R.P.F. Gomes, M.F.P. Lopes, J.C.C. Henriques, L.M.C. Gato, A.F.O.
881 Falcao (2015) The dynamics and power extraction of bottom-hinged
882 plate wave energy converters in regular and irregular waves. *Ocean En-*
883 *gineering*, Vol. 96, pp. 86-99
- 884 [39] A. Pecher, J.P. Kofoed, J. Espedal, S. Hagberg (2010) Results of an
885 Experimental Study of the Langlee Wave Energy Converter. In Proc.
886 Of the 20th International Offshore and Polar Engineering Conference,
887 Beijing, China
- 888 [40] J. Lavelle, J.P. Kofoed (2011) Experimental testing of the Langlee Wave
889 Energy Converter. In Proc. Of the 9th European Wave and Tidal Energy
890 Conference, Southampton, UK
- 891 [41] E. Angelelli, B. Zanuttigh, J.P. Kofoed, K. Glejbol (2011) Experiments
892 on the WavePiston Wave Energy Converter, Proc. Of the 9th European
893 Wave and Tidal Energy Conference, Southampton, UK
- 894 [42] J. Cordonnier, F. Gorintin, A. De Cagny, A.H. Clement, A. Babarit
895 (2015) SEAREV: case study of the development of a wave energy con-
896 verter. *Renewable Energy* (Accepted for publication)

- 897 [43] Rendel Palmer & Tritton and Kennedy & Donkin (1982) United King-
898 dom Wave Energy Program - Consultants' 1981 Assessment. Depart-
899 ment of Energy, UK
- 900 [44] Y-H. Yu, Y. Li, K. Hallett, C. Hotimsky (2014) Design and analysis for
901 a floating oscillating surge wave energy converter. In Proc. Of the 33rd
902 International Conference on Ocean, Offshore and Arctic Engineering, San
903 Francisco, California, USA
- 904 [45] Y. Kamizuru (2014) Development of hydrostatic drive trains for wave
905 energy converters. PhD thesis, Aachen University.
- 906 [46] J. Falnes (1975) A resonant point absorber of ocean-wave power. *Nature*,
907 Vol. 256, pp. 478-479
- 908 [47] A. Babarit, A.H. Clement (2009) Application of the optimal command
909 method to the control of the SEAREV wave energy converter: a study on
910 the influence of time constants on the efficiency of the latching control.
911 In Proc of the 9th European Control Conference, Budapest, Hungary
- 912 [48] J. Cretel, A.W. Lewis, G. Thomas, G. Lightbody (2011) A critical as-
913 sessment of latching as control strategy for wave-energy absorbers. In
914 Proc. of the 31st International Offshore and Polar Engineering Confer-
915 ence, Hawaii
- 916 [49] R. Genest, F. Bonnefoy, A.H. Clement, A. Babarit (2014) Effect of non
917 ideal power take off on the energy absorption of a reactively controlled
918 one degree of freedom wave energy converter. *Applied Ocean Research*,
919 Vol. 48, pp. 236-243
- 920 [50] D.V. Evans (1976) A theory for wave-power absorption by oscillating
921 bodies. *Journal of Fluid Mechanics* Vol. 77(1), pp. 1-25
- 922 [51] P. Stansell, D.J. Pizer (2011) Maximum wave-power absorption by at-
923 tenuating line absorbers under volume constraints. Cornwell University
924 Library.
- 925 [52] J.M. Grases (2013) MARINET Infrastructure Access Report. Infrastruc-
926 ture: IFREMER Deep Seawater Wave Tank. User-project: SDK Wave
927 Turbine

- 928 [53] D.D. Prasad, M.R. Ahmed, Y-H. Lee (2014) Flow and performance char-
929 acteristics of a direct drive turbine for wave power generation. *Ocean*
930 *Engineering*, Vol. 81, pp. 39-49
- 931 [54] F.J.M. Farley, R.C.T. Rainey, J.R. Chaplin (2012) Rubber tubes in the
932 sea. *Philosophical transactions of the royal society A*, Vol. 370, pp. 381-
933 402
- 934 [55] A. Babarit, B. Gendron, J. Singh, C. Mélis, P. Jean (2013) Hydro-
935 elastic modelling of an electro-active wave energy converter. In *Proc. of*
936 *the 32nd International Conference on Ocean, Offshore and Artic Engi-*
937 *neering*, Nantes, France
- 938 [56] Ramboll, Dansk Hydraulisk Institut, Danmarks meteorologiske institut
939 (1999) Kortlægning af bolgeenergiforhold i den Danske del af nordsoean.
940 Technical report. *In Danish*
- 941 [57] T. Verdel (2007) *Décision et prévision statistiques. Chapitre 7: la*
942 *régression linéaire. Lecture notes of Ecole des Mines de Nancy. In French*
- 943 [58] K. Gunn, C. Stock-Williams (2012) Quantifying the global wave power
944 resource. *Renewable Energy*, Vol. 44, 296-304